Supporting Information

Sachs et al. 10.1073/pnas.1204614110

SI Materials and Methods

Animal Experiments. To induce short-term hyperproliferation, mice were treated with a single dose of 12.34 μg 12-*O*-tetradecanoylphorbol-13-acetate (TPA) and killed 24 h later or with a single dose of 30 μg 7,12-dimethylbenzanthracene (DMBA) followed by four semiweekly doses of 12.34 μg TPA and killed 3 d later. To induce nuclear translocation of Cre-PGR in *Itga3*$^{tm1Son/tm1Son}$*; mTmG*$^{+/-}$*; Tg(Krt1-15-cre/PGR)22Cot* mice, we applied generous portions of 100 mg RU486 (Sigma), dissolved in 5 mL ethanol and mixed with 10 g hand cream (Neutrogena), to the shaved back skin of telogen mice through ages 20–25 d with cotton swaps (~2 mg RU486 per application). For s.c. tumor growth, 50,000 cells in 150 μL PBS were injected s.c. in either flank of athymic *nu/nu* BALB/c mice. Mouse hair was dyed with permanent coloring shampoo (L'Oreal) at 3 and 8 wk of age and photographed weekly to track anagen hair cycles. In addition, hair cycle phases were classified histologically according to ref. 1. To induce hair follicle (HF) depletion, mice were treated semiweekly with 12.34 μg TPA in 200 μL acetone (or acetone only) from weeks 7 to 30, shaved, and photographed. To determine rates of epidermal turnover, the backs of adult mice were shaved, topically treated with 12.34 μg TPA, i.p. injected with 100 μg BrdU/g body weight, and chased for 14 d. Alternatively, 5% (wt/vol) dansyl chloride in Nivea Hydratant Body Milk was thoroughly applied to mouse backs 24 h after shaving. Cages were maintained in shaded areas over the whole experiment. Animals were killed, and the back skin was isolated and processed for immunofluorescence. Dansyl chloride was excited with a 405-nm laser line and quantified using ImageJ. All animal studies were performed according to Dutch guidelines for care and use of laboratory animals and were approved by the appropriate animal welfare committee (Dier Experiment Commissie of The Netherlands Cancer Institute).

To analyze *Hras1* mutations, genomic DNA was isolated from papillomas using the QIAamp DNA Mini Kit (Qiagen). Sequences flanking codon 61 of *Hras1* was amplified by nested PCR [3 min, 94 °C; 35× (30 s, 94 °C; 30 s, 45 °C; 30 s, 72 °C); 5 min 72 °C]: PCR 1 (forward 5′-TAGGTGGCTCACCTGTACTG-3′ and reverse 5′-CGTTGAATTCTCTGGTCTGAGGA-3′) generated a 267-bp product. PCR 2 (forward 5′-GGAACTTGGTGTTGTTGATGGC-3′ and reverse 5′-CTAAGCCTGTTGTTTTGCAGGAC-3′) generated a second 177-bp product, of which 5–10 μg was digested with XbaI overnight at 37 °C. Fragments were analyzed by 2.5% (wt/vol) agarose gel electrophoresis and stained with ethidium bromide. The 177-bp product was sequenced with primer set 2 and the BigDyeTerminator v3.1 Cycle Sequencing Kit following the manufacturer's instructions.

Microarray analysis was performed on mRNA isolated from the interfollicular epidermis (IFE) of three WT and two epidermal-specific *Itga3* knockout mice (*Itga3* eKO) using platform Illumina WholeGenome-6-Version 2 mouse bead arrays.

Immunohistochemistry. Tissues were excised, fixed 1 d in formaldehyde, embedded in paraffin, sectioned, and stained [H&E, immunohistochemistry (IHC)]. Images were taken with PL APO objectives (10×/0.25 NA, 40×/0.95 NA, and 63×/1.4 NA oil) on an Axiovert S100/AxioCam HR color system using AxioVision 4 software (Carl Zeiss MicroImaging) or with a 20×/0.75 NA PL APO objective ± a 2× optical mag changer on a ScanScope XT system using ImageScope v10 software (Aperio Technologies). Tumor classification and grading were performed blindly.

Immunofluorescence and Whole Mounts. Skin was excised and embedded in cryoprotectant [Tissue-Tek OCT (optimal cutting temperature) compound]. Cryosections were prepared, fixed in ice-cold acetone, and blocked with 2% (wt/vol) BSA in PBS. To prepare epidermal whole mounts, tail skin was cut into 0.5-cm-wide pieces and incubated in 5 mM EDTA in PBS at 37 °C for 4 h. An intact sheet of epidermis was gently peeled away from the dermis and fixed in 4% (vol/vol) paraformaldehyde in PBS for 2 h at room temperature. Fixed epidermal sheets were permeabilized and blocked in PB buffer [20 mM Hepes buffer, pH 7.2, containing 0.5% (vol/vol) TritonX-100, 0.5% (wt/vol) skim milk powder, and 0.25% (vol/vol) fish skin gelatin] and incubated with 2 M HCl at 37 °C for 25 min when necessary (anti-BrdU stainings). Tissues were incubated with the indicated primary antibodies in 2% (wt/vol) BSA in PBS (whole mounts: PB buffer) for 60 min (whole mounts: overnight), followed by incubation with secondary antibodies diluted 1:200 for 60 min (whole mounts: overnight). 5-ethynyl-2-deoxyuridine (EdU) was detected using the Click-iT system according to the manufacturer's instructions (Invitrogen). Samples were analyzed at 37 °C using a 20 63×/1.4 HCX PL APO CS oil objective on a TCS SP2 AOBS confocal microscope (Leica Microsystems). Images were acquired using LCS 2.61 (Leica Microsystems) and processed using Adobe Photoshop CS4 or ImageJ.

Cell Lines. All cell lines were grown at 37 °C in a humidified atmosphere of 5% (vol/vol) CO_2 in air. Mouse keratinocyte (MK) *Itga3*$^{fl/fl}$ and MK *Itga3*$^{-/-}$ were generated as described (2) and grown in supplemented keratinocyte serum-free medium. For single cell migration, cells were seeded on a laminin-332 rich matrix deposited by Rac11-P cells (3), starved overnight, and treated with 10 nM TPA. Cells were imaged every 8 min with an Axiocam CCD camera using a 10×/0.25 Achroplan Ph1 objective on an Axiovert S100 wide-field system (Zeiss) and analyzed using MatLab software as described (4). Adhesion strengthening experiments were performed on a home-built spinning disk machine as previously described (5, 6). Cells (5×10^6) were seeded on 30-mm glass coverslips coated with a laminin-332 rich matrix deposited by Rac11-P cells. Twenty-four hours later, they were exposed to a varying range of shear stresses in PBS for 8 min at room temperature, fixed in 2% (vol/vol) paraformaldehyde, stained with DAPI, and imaged with a Hamamatsu ORCA-ER BW CCD camera on an automated AxioObserver Z1 inverted microscope (Zeiss) using a 5×/0.15 Plan-Neofluar. Cell detachment as function of shear stress was quantified using ImageJ and plotted using SigmaPlot 11 (Systat). Murine skin cancer cell lines P1, B9, and A5 were cultured as described (7, 8). Stable *Itga3* knockdown P1 cells were generated by lentiviral transduction of short RNA hairpins cloned into pLKO.1 vectors (clone 1: TRCN0000065998; clone 2: TRCN0000066002; Thermo Scientific Dharmacon RNAi Technologies) and FACS sorted three times for negative expression of integrin α3. To allow spheroid formation, 10,000 cells were seeded in DMEM [10% (vol/vol) FCS, 2% (vol/vol) matrigel] in 24-well plates coated with growth factor–reduced matrigel (BD). Phase-contrast images were acquired after 10 d on an Axiovert 200m Zeiss microscope with a Zeiss Axiocam MRm camera. Area was measured with ImageJ and converted to volume assuming a spheroid shape. Eight-micrometer pore size Boyden Chambers (Costar) were coated with 1:5 growth factor–reduced matrigel dilution in serum-free DMEM, and 100,000 cells were seeded in DMEM [1% (vol/vol) FCS]. Chambers were transferred to a 24-well plate containing

600 μL DMEM [10% (vol/vol) FCS]. Cells were allowed to migrate for 16 h, washed with PBS, fixed in 2% PFA, and stained with crystal violet. Cells on the upper side of the membrane were removed with a cotton swab, the remaining migrated cells were solubilized in 1% (vol/vol) SDS, and the absorbance of crystal violet at 550 nm was read in a iMark microplate reader (Bio-Rad). Mouse squamous carcinoma cell (MSCC) *Itga3*$^{fl/fl}$ were isolated from the sentinel lymph node of an squamous cell carcinoma (SSC) on a DMBA/TPA-treated *Itga3*$^{fl/fl}$ mouse by mechanical disruption, followed by collagenase digestion and culture in DMEM containing 10% (vol/vol) FCS (Gibco). α3 was deleted using Adeno-Cre (9) to generate MSCC *Itga3*$^{-/-}$.

Immunoblotting. For biochemical assays, epidermis/cells were lysed in 1% (vol/vol) Nonidet P-40, 20 mM Tris-HCl, pH 7.6, 4 mM EDTA, and 100 mM NaCl, supplemented with a mixture of protease inhibitors (P8340; Sigma). Lysates were cleared by centrifugation for 20 min at 20,000 × *g* and 4 °C, followed by separation of proteins on 4–12% (vol/vol) polyacrylamide gels under nonreducing conditions (NuPage) and transferred to Immobilon PVDF membranes (EMD Millipore).

FACS. Cells were trypsinized, washed with 2% (vol/vol) FCS in PBS, and stained with primary antibodies as indicated for 60 min on ice. After washing, secondary anti-goat, -rat, and -mouse antibodies coupled to FITC were used 1:200 for 60 min on ice. Cells were strained and analyzed on a 1998 BD FACSCalibur (Becton Dickinson) using a 488-nm laser and a 530/30 FL1 filter configuration.

1. Müller-Röver S, et al. (2001) A comprehensive guide for the accurate classification of murine hair follicles in distinct hair cycle stages. *J Invest Dermatol* 117(1):3–15.
2. Margadant C, et al. (2009) Integrin alpha3beta1 inhibits directional migration and wound re-epithelialization in the skin. *J Cell Sci* 122(Pt 2):278–288.
3. Delwel GO, et al. (1993) Expression and function of the cytoplasmic variants of the integrin alpha 6 subunit in transfected K562 cells. Activation-dependent adhesion and interaction with isoforms of laminin. *J Biol Chem* 268(34):25865–25875.
4. Loerke D, et al. (2012) Quantitative imaging of epithelial cell scattering identifies specific inhibitors of cell motility and cell-cell dissociation. *Sci Signal* 5(231):rs5.
5. Boettiger D (2007) Quantitative measurements of integrin-mediated adhesion to extracellular matrix. *Methods Enzymol* 426:1–25.
6. Sachs N, et al. (2012) Blood pressure influences end-stage renal disease of Cd151 knockout mice. *J Clin Invest* 122(1):348–358.
7. Burns PA, et al. (1991) Loss of heterozygosity and mutational alterations of the p53 gene in skin tumours of interspecific hybrid mice. *Oncogene* 6(12):2363–2369.
8. Haddow S, Fowlis DJ, Parkinson K, Akhurst RJ, Balmain A (1991) Loss of growth control by TGF-beta occurs at a late stage of mouse skin carcinogenesis and is independent of ras gene activation. *Oncogene* 6(8):1465–1470.
9. Anton M, Graham FL (1995) Site-specific recombination mediated by an adenovirus vector expressing the Cre recombinase protein: a molecular switch for control of gene expression. *J Virol* 69(8):4600–4606.

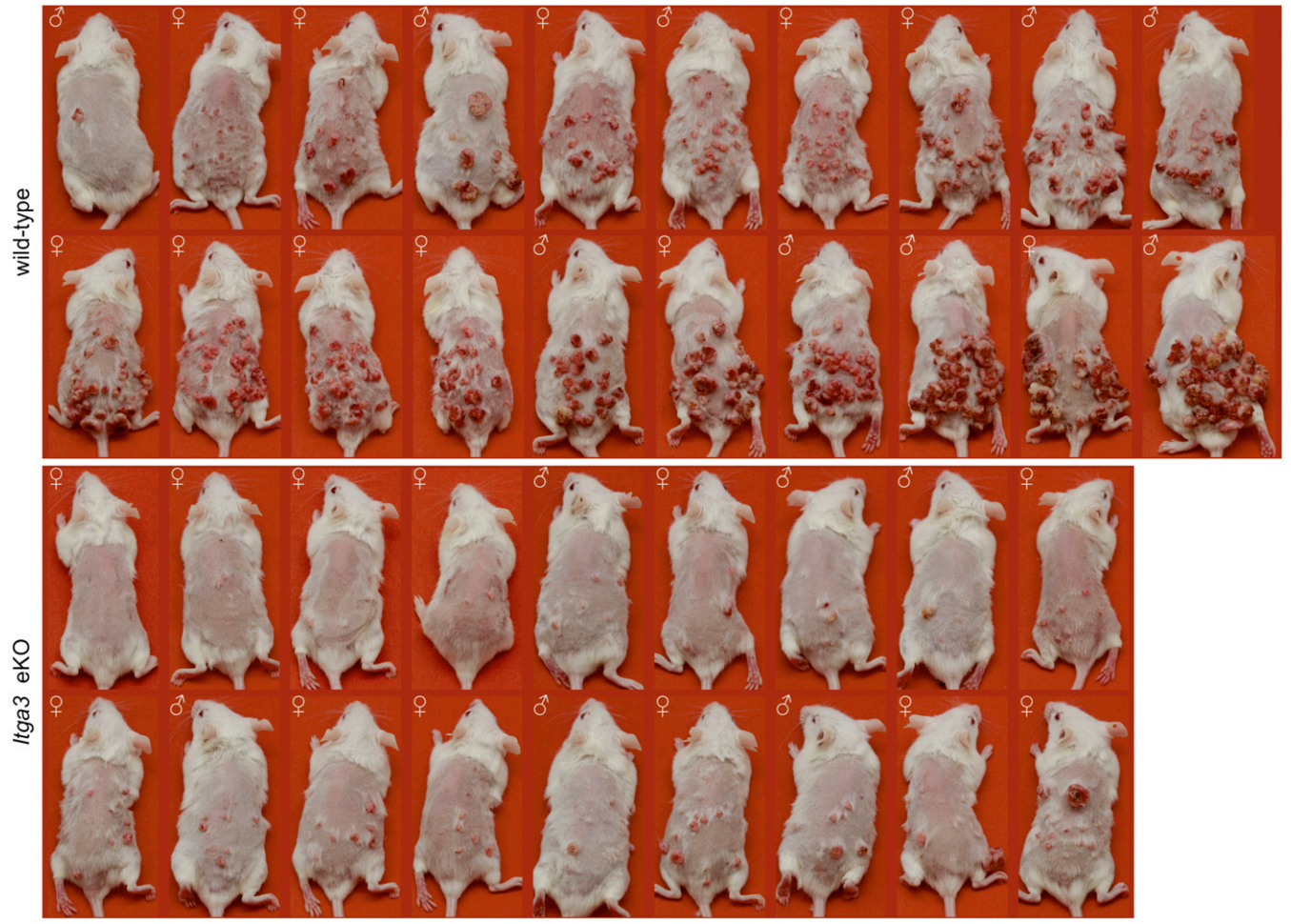

Fig. S1. WT and Itga3 eKO mice at the end of the DMBA/TPA regimen. Most mice used for the quantification in Fig. 1*B* are shown according to total tumor volume (20/22 WT, 18/18 *Itga3* eKO).

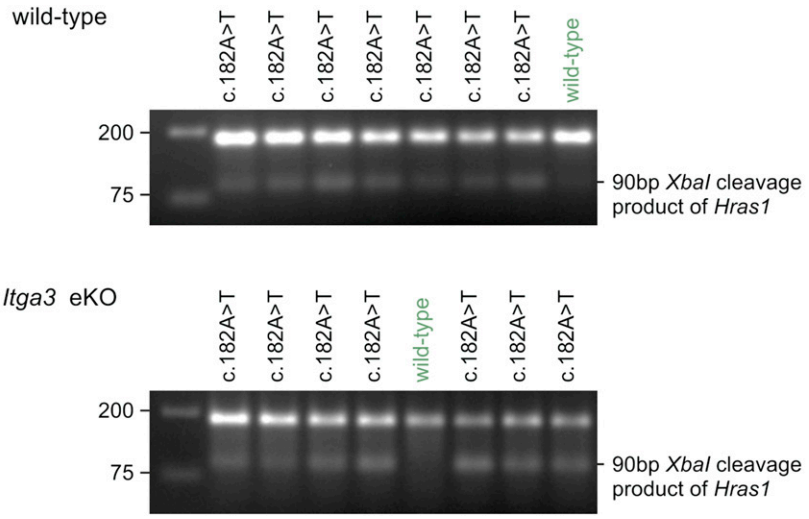

Fig. S2. Restriction fragment length analysis of the *Hras1* proto-oncogene amplified from the genomic DNA of WT and *Itga3* eKO papillomas. In the majority of papillomas, DMBA/TPA treatment causes an XbaI cleavage site. The underlying point mutation c.182A > T in codon 61 of *Hras1* has been confirmed by direct sequencing.

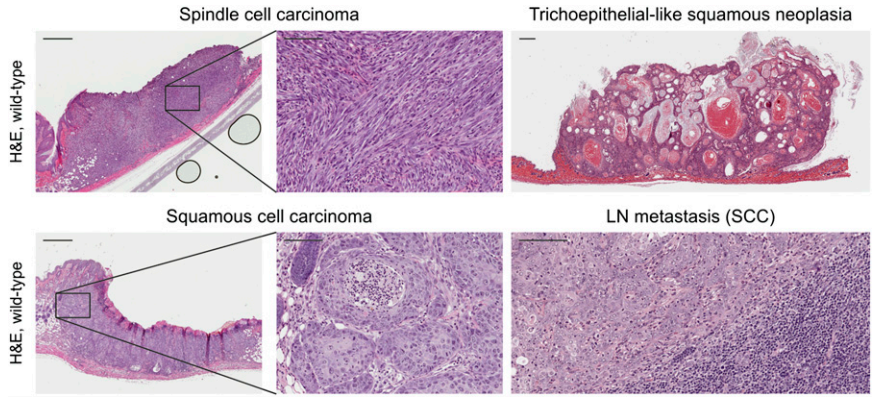

Fig. S3. Histological examples of DMBA/TPA-promoted malignant tumors found in WT mice: spindle cell carcinoma, trichoepithelial-like squamous neoplasia, and metastasizing squamous cell carcinoma [Scale bars, 500 (overviews) and 100 μm (magnifications).]

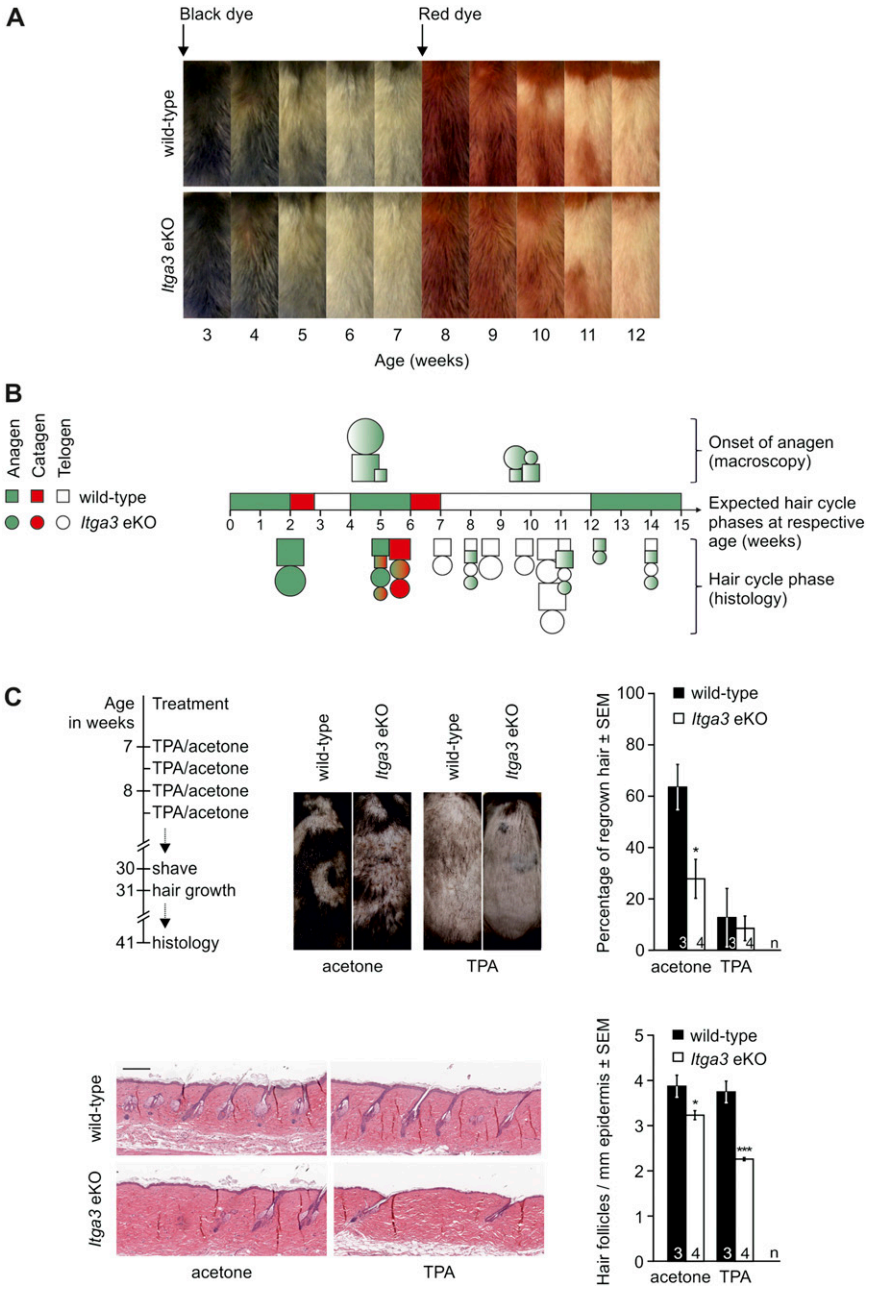

Fig. S4. Analysis of hair cycle and growth in WT and *Itga3* eKO mice. (*A*) The dorsal hair of WT and *Itga3* eKO mice was dyed twice during telogen. Outgrowing white hair marks the onset of anagen. (*B*) Quantification of *A* shows no phase shift in the onset of hair cycles II and III between the two groups. In addition, hair cycle phases are synchronized in age-matched WT and *Itga3* eKO mice based on histological classification. The expected time scale of hair cycle phases is based on Müller-Rover et al. (1), and the area of boxes/circles is proportional to the number of mice (smallest unit in legend equals $n = 1$). (*C*) Long-term TPA treatment or deletion of epidermal *Itga3* causes delayed hair growth and depletion of hair follicles in old C57BL/6 mice. (*Upper*) Experimental setup, representative macroscopic photographs 1 wk after shaving and quantification of macroscopic hair growth. (*Lower*) Representative microscopic images and quantification of hair follicle density 11 wk after shaving ($*P < 0.05$, $***P < 0.001$). (Scale bar, 200 μm.)

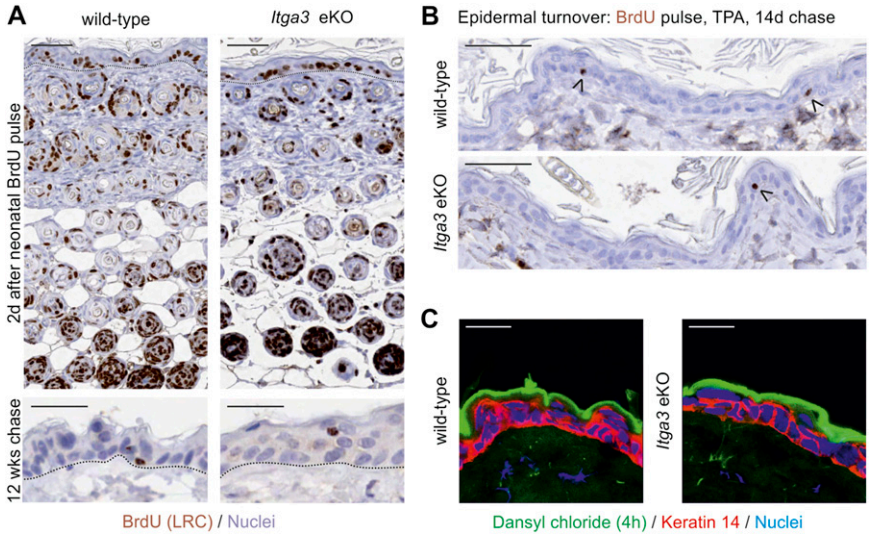

Fig. S5. Representative histological examples of BrdU pulse-chase and dansyl chloride desquamation experiments. (*A*) An equal number of keratinocytes in neonatal WT and *Itga3* eKO mice was labeled with BrdU (*Upper*). After a 12-wk chase period, suprabasal BrdU-positive cells are regularly observed only in *Itga3* eKO mice. [Scale bars, 200 (*Upper*) and 50 μm (*Lower*).] (*B*) Fewer BrdU-positive cells are present 14 d after labeling in *Itga3* eKO mice. (Scale bar, 100 μm.) (*C*) Dansyl chloride labels the uppermost epidermal layer. (Scale bar, 20 μm.)

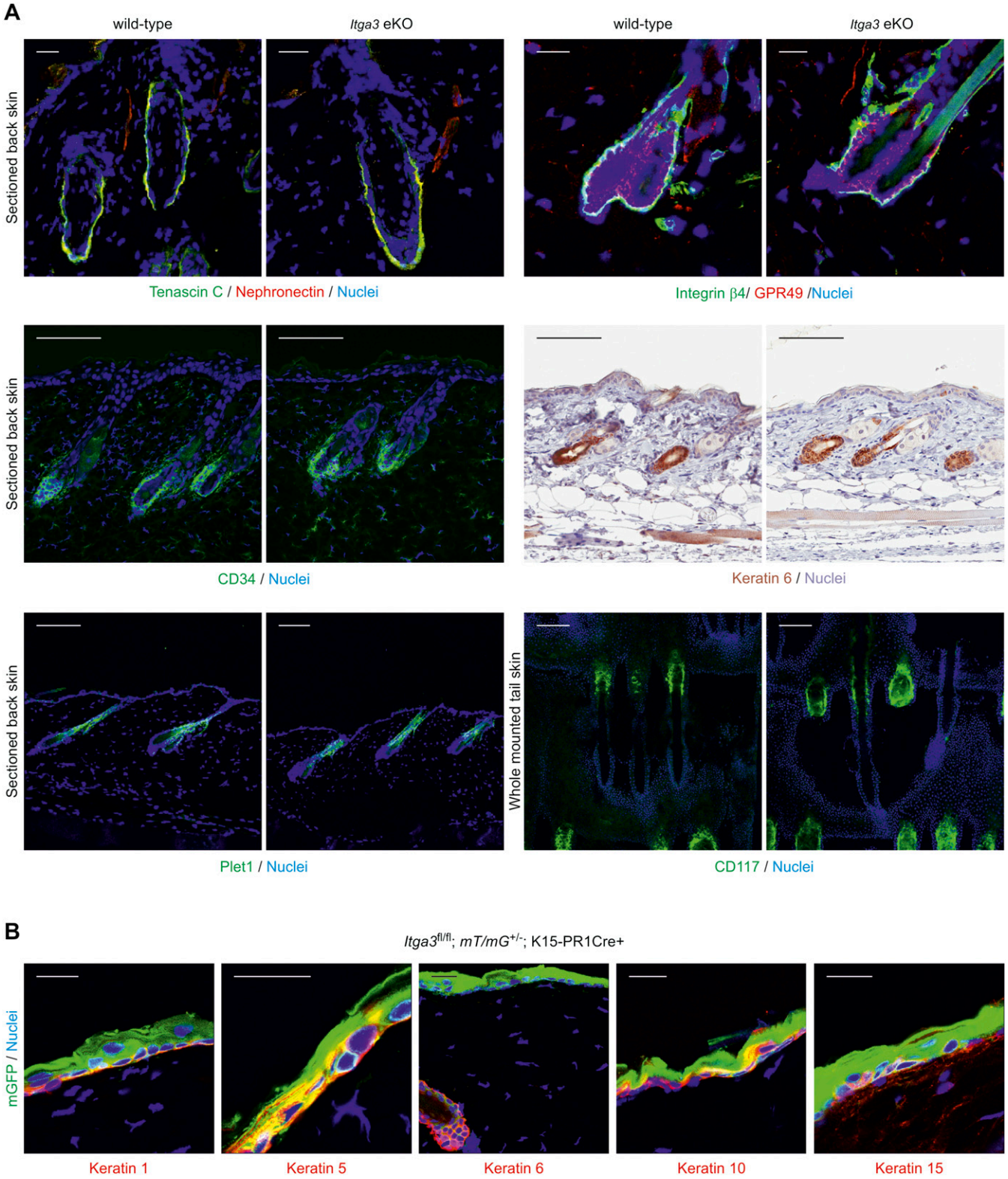

Fig. S6. Immunofluorescent analysis of WT and *Itga3* eKO HFs and differentiation markers in GFP$^+$ cells from *Itga3*$^{fl/fl}$; *mTmG*$^{+/-}$; *Krt1-15-CrePR1+* mice. (*A*) Several HF markers are similarly distributed in the skin of WT and *Itga3* eKO mice as shown by immunofluorecent and immunohistochemical stainings: tenascin-C, nephronectin, GPR49 (Lgr5), CD34, and keratin 6 are localized in the bulge; Plet1 is localized in the isthmus; CD177 (c-kit) is localized in the infundibulum. [Scale bars, 20 (*Top*) and 100 μm (*Middle* and *Bottom*).] (*B*) Immunofluorescent analysis of *Itga3*$^{fl/fl}$; *mTmG*$^{+/-}$; *K15-PR1Cre+* skin shows that all layers of the IFE contain GFP-positive progeny, which express keratins 1, 5, 10, and 15 but not 6. (Scale bar, 20 μm.)

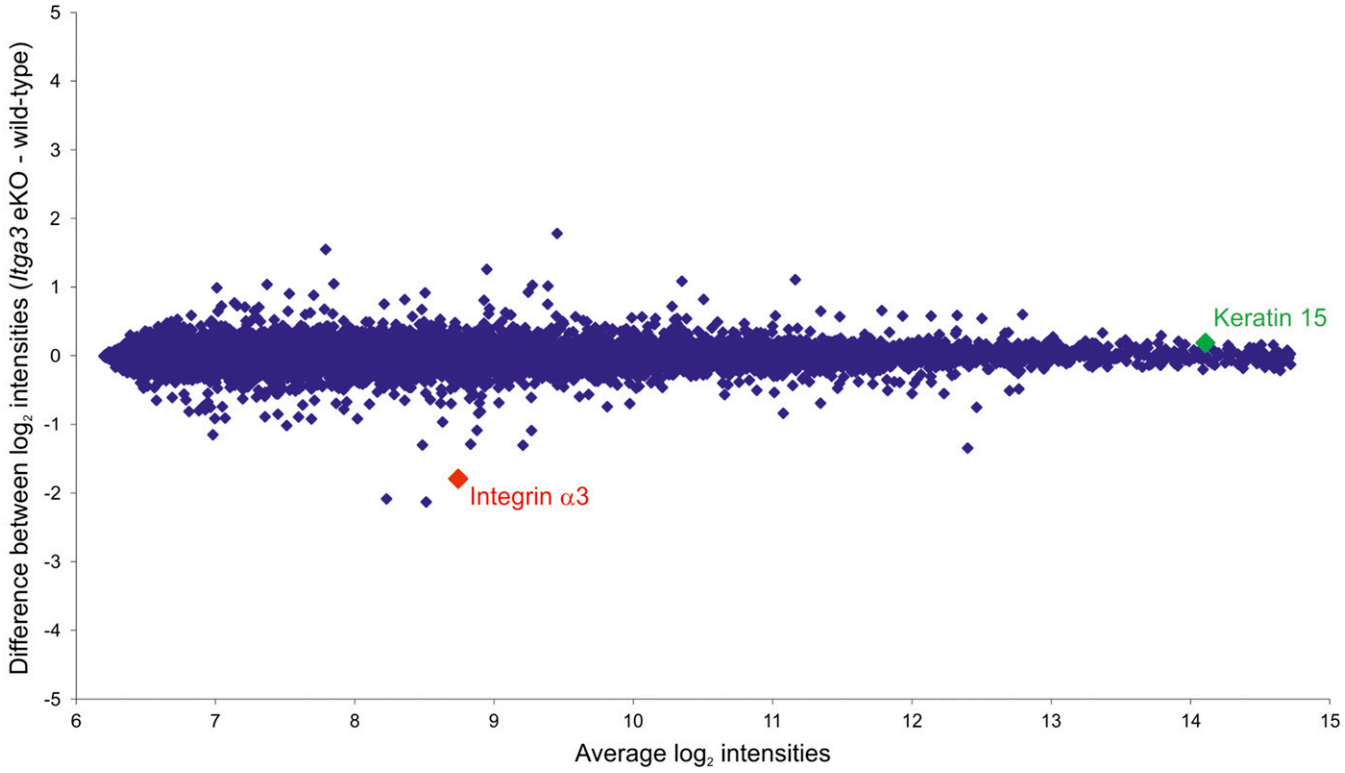

Fig. S7. Normalized MA-plot for a microarray comparing mRNA from the IFE of three WT and two *Itga3* eKO mice. The spots corresponding to *Itga3* (integrin a3) and *Krt15* (keratin 15) are highlighted.

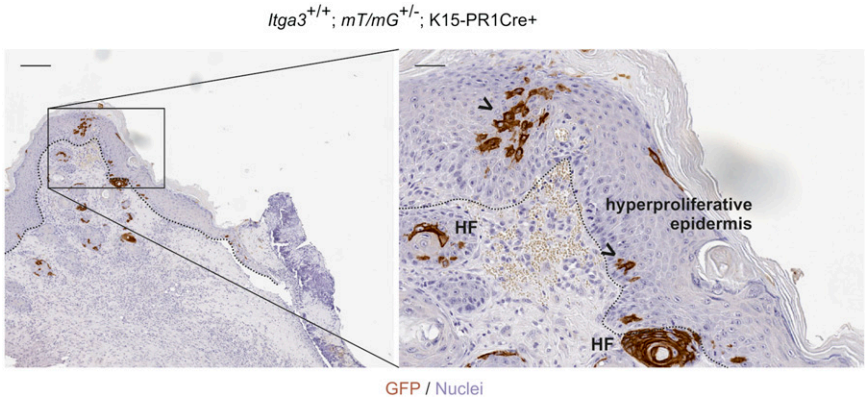

Fig. S8. K15-Cre–mediated recombination of the *mTmG* allele leads to GFP expression in HFs as recognized by immunohistochemistry. GFP-positive cells (>) are also found in the hyperproliferative epidermis closing a wound inflicted by an asocial littermate 2 d earlier, demonstrating that HF bulge cells contribute to reepithelialization after wounding. [Scale bars, 200 (overview) and 50 μm (magnification).]

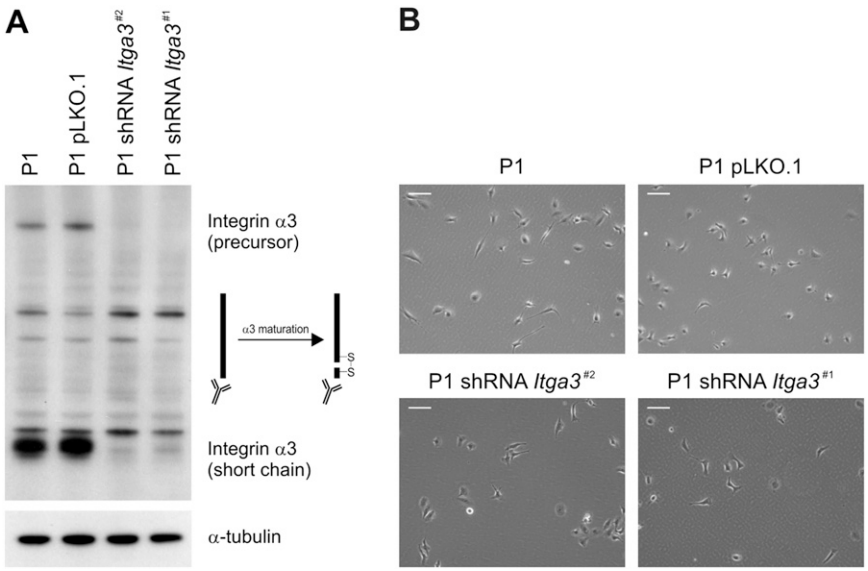

Fig. S9. Characterization of P1 cells ± *Itga3*. (*A*) Western blot showing the virtual absence of integrin α3 from lysates of P1 cells carrying lentiviral shRNA constructs against *Itga3*. P1 cells carrying the control construct pLKO.1 have unaltered α3 levels comparable to the parental cell line P1. (*B*) Phase contrast images of P1, control, and *Itga3* knockdown cells. (Scale bar, 100 μm.)

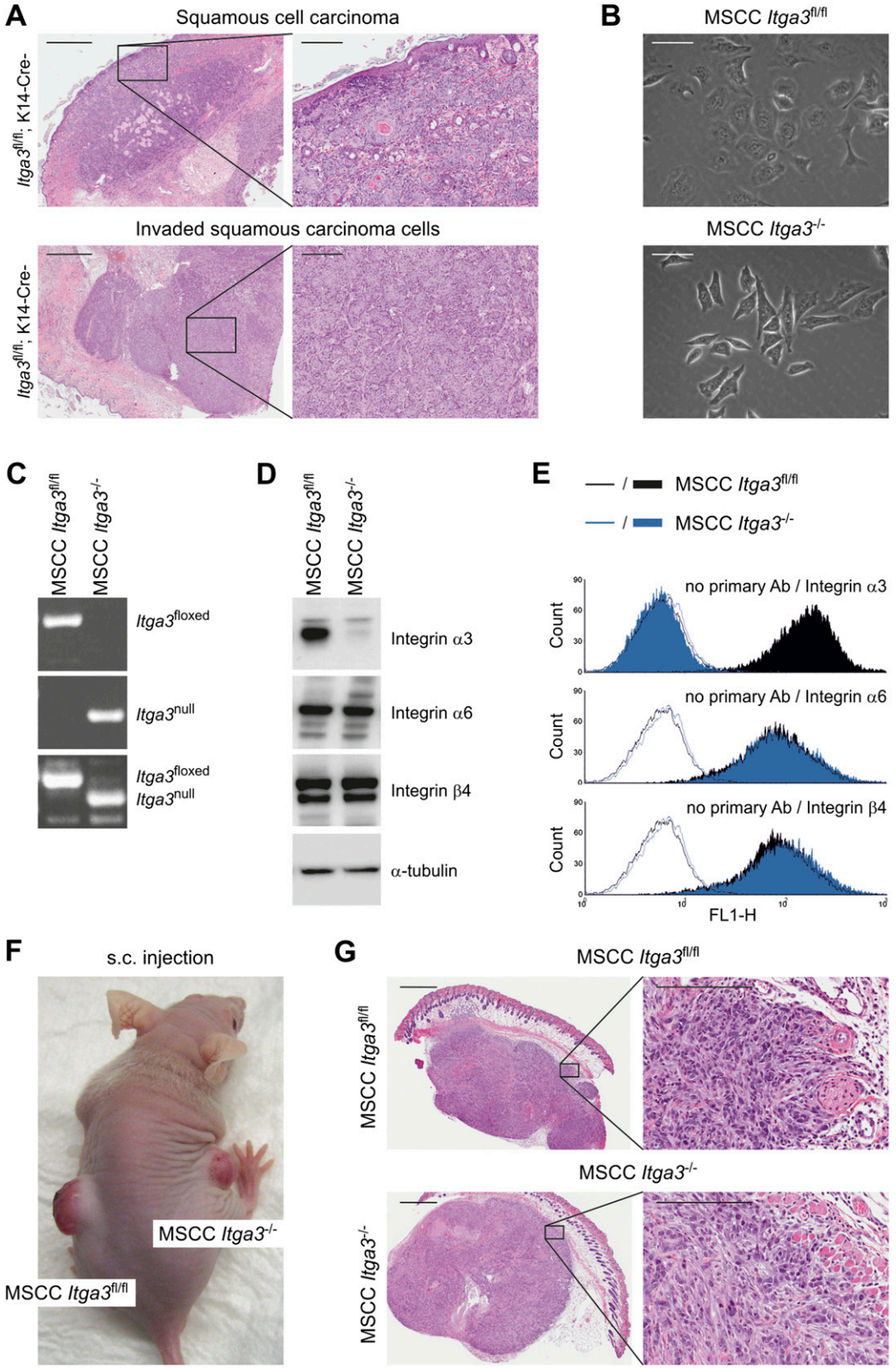

Fig. S10. Characterization of MSCCs ± *Itga3*. (*A*) Invading SCCs of a DMBA/TPA-treated *Itga3*$^{fl/fl}$ mouse. [Scale bars, 1 mm (overviews) and 200 μm (magnifications).] (*B*) Phase contrast images depicting parental cell line MSCC *Itga3*$^{fl/fl}$ isolated from invading SCC (*A*) and daughter cell line MSCC *Itga3*$^{-/-}$ obtained after Cre-mediated recombination in vitro. Parental MSCC *Itga3*$^{fl/fl}$ cells are flat and grow in islands, whereas MSCC *Itga3*$^{-/-}$ cells have a more contractile and migratory phenotype. (Scale bar, 50 μm.) (*C*) Recombination of both *Itga3* alleles in MSCC *Itga3*$^{-/-}$, but not MSCC *Itga3*$^{fl/fl}$, cells as determined by PCR on genomic DNA. (*D*) Western blot analysis of integrins α3, α6, and β4. Whereas α3 is absent in MSCC *Itga3*$^{-/-}$ cells, expression of α6 and β4 remains unaltered. (*E*) FACS analysis of α3, α6, and β4. Whereas α3 is absent in MSCC *Itga3*$^{-/-}$ cells, cell surface expression of α6 and β4 remains unaltered. (*F*) Representative nude mouse with tumors originating from MSCC *Itga3*$^{fl/fl}$ (left flank) and MSCC *Itga3*$^{-/-}$ cells (right flank, smaller tumor) 4 wk after s.c. injection. (*G*) s.c. tumors originating from MSCC *Itga3*$^{fl/fl}$ and MSCC *Itga3*$^{-/-}$ cells show equally poor differentiation.

A

	wild-type		*Itga3* eKO	
	n	%	n	%
Well differentiated SCC	14	26%	4	12%
Moderately differentiated SCC	33	62%	15	45%
Poorly differentiated SCCs and others	6	11%	14	42%
Poorly differentiated SCC	(6)	(11%)	(12)	(36%)
Spindle cell carcinoma	(0)	(0%)	(1)	(3%)
Anaplastic carcinoma	(0)	(0%)	(1)	(3%)

B

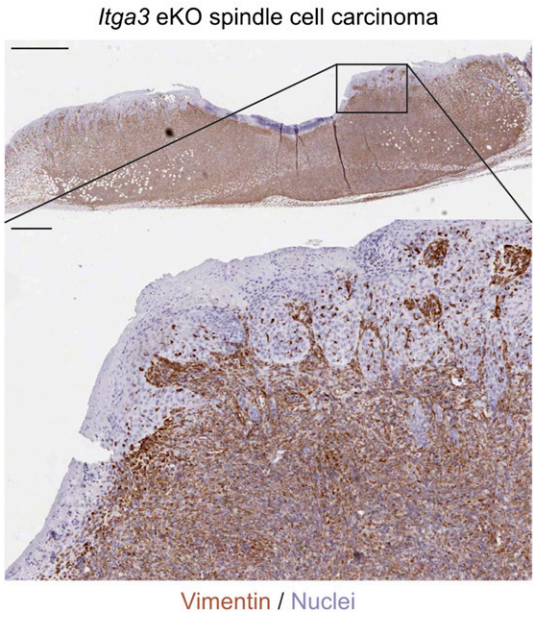

Fig. S11. (*A*) Detailed grading of skin tumors of WT and *Itga3* eKO mice subjected to the DMBA protocol. The difference in malignancy grades between WT and *Itga3* eKO mice is statistically significant ($P < 0.001$; χ^2 test). (*B*) Vimentin staining on the spindle cell carcinoma found in a DMBA-treated *Itga3* eKO mouse [Scale bars, 1 mm (overview) and 100 μm (magnification).]

Table S1. List of antibodies used including application, dilution, and source

Antigen	Name	Type	Application	Dilution	Company	Ref(s).
BrdU	MO744	Mouse mAb	IHC/IF	1:100	DakoCytomation	
CD117	135107	Rat mAb	IF	1:100	Biolegend	
CD34	MA1-22646	Rat mAb	IF	1:200	Pierce	
E-cadherin	36/E-cadherin	Mouse mAb	WB	1:1,000	BD Biosciences	
GFP	ab6556	Rabbit pAb	IHC	1:400	Abcam	
GPR49	AJ1330a	Rabbit mAb	IF	1:100	Abcam	
Itga3	AF2787	Goat pAb	FACS	1:100	R&D Systems	
Itga3	141742	Rabbit pAb	WB	1:1,000		(1)
Itga6	GoH3	Rat mAb	FACS/IF	Undiluted		(2)
Itga6	AA6NT	Rabbit pAb	WB	1:5,000		(3)
Itgb4	346-11A	Rat mAb	FACS/IF	1:200	BD Biosciences	
Itgb4	β4Ares1115-1355	Rabbit pAb	WB	1:5,000		(4)
Ki67	PSX1028	Rabbit pAb	IHC	1:750	Monosan	
Krt1	PRB-165P	Rabbit pAb	IF	1:200	Covance	
Krt5	PRB-160P	Rabbit pAb	IF	1:200	Covance	
Krt6	PRB-169P	Rabbit pAb	IHC/IF	1:200	Covance	
Krt10	PRB-159P	Rabbit pAb	IF	1:200	Covance	
Krt14	PRB-155P	Rabbit pAb	IF	1:400	Covance	
Krt15	MA1-90929	Mouse mAb	IHC/IF	1:200	Thermoscientific	
Nephronectin	AF4298	Goat pAb	IF	5 μg/mL	R&D Systems	
Plet1	33A10	Rat mAb	IF	1:200		(5)
Tenascin-C	LAT-2	Rat mAb	IF	Undiluted		(6)
Tubulin	B-5-1-2	Mouse mAb	WB	1:5,000	Sigma	
Vimentin	9661L	Rabbit pAb	IHC	1:200	Cell Signaling	

IF, immunofluorescence; IHC, immunohistochemistry; WB, Western blotting; FACS, fluorescence-activated cell sorting.

1. Sachs N, et al. (2006) Kidney failure in mice lacking the tetraspanin CD151. *J Cell Biol* 175(1):33–39.
2. Sonnenberg A, Janssen H, Hogervorst F, Calafat J, Hilgers J (1987) A complex of platelet glycoproteins Ic and IIa identified by a rat monoclonal antibody. *J Biol Chem* 262(21): 10376–10383.
3. Ports MO, Nagle RB, Pond GD, Cress AE (2009) Extracellular engagement of alpha6 integrin inhibited urokinase-type plasminogen activator-mediated cleavage and delayed human prostate bone metastasis. *Cancer Res* 69(12):5007–5014.
4. Wilhelmsen K, et al. (2007) Serine phosphorylation of the integrin beta4 subunit is necessary for epidermal growth factor receptor induced hemidesmosome disruption. *Mol Biol Cell* 18 (9):3512–3522.
5. Sonnenberg A, et al. (1993) Formation of hemidesmosomes in cells of a transformed murine mammary tumor cell line and mechanisms involved in adherence of these cells to laminin and kalinin. *J Cell Sci* 106(Pt 4):1083–1102.
6. van der Flier A, et al. (1997) Spatial and temporal expression of the beta1D integrin during mouse development. *Dev Dyn* 210(4):472–486.